A New Experimental Technique for Applying Impulse Tension Loading

Z. S. Fan[1], H. P. Yu[1,2*], H. Su[3], X. Zhang[1], C. F. Li[1]

[1] National Key Laboratory for Precision Hot Processing of Metals, Harbin Institute of Technology, China;
[2] School of Materials Science and Engineering, Harbin Institute of Technology, China;
[3] Tianjin Long March Launch Vehicle Manufacturing Co.Ltd., China
[*]Corresponding author. Email: haipingy@hit.edu.cn; Tel.: +86 451 8641 8753

Abstract

This paper deals with a new experimental technique for applying impulse tension loads. Briefly, the technique is based on the use of pulsed-magnetic-driven tension loading. Electromagnetic forming (EMF) can be quite effective in increasing the forming limits of metal sheets, such as aluminium and magnesium alloys. Yet, why the forming limit is increased is still an open question. One reason for this is the difficulty to let forming proceed on a certain influence monotonically: the main phenomena causing this increase in formability are considered to due to "body force" effect, inertia effect, changes in strain rate sensitivity. In this study, an impulse tension loading setup is presented. "Body force" effect and strain rate, which are known to be the two key factors leading to higher formability, can now be separated freely by our designed device. Reproducible and adjustable loading rate (80s-1~3267s-1) can be achieved by adjusting the discharge voltage and capacitance. The relation between the discharge voltage and strain rate was obtained with the help of finite element calculations and high-camera measurement results. The results of an exploratory experiment carried out on the designed device are presented for aluminum alloy AA5052 sheet. It shows that this technique could be used to study the dynamic response of sheets.

Keywords

Electromagnetic forming, Forming limit, Tension loading

1 Introduction

Electromagnetic forming (EMF) is high potential process for sheet metal forming, as it offers many advantages such as higher formability. Yet, why the forming limit is increased is still an open question. One reason for this is the difficulty to let forming proceed on a certain influence monotonically: the main phenomena causing this increase in formability are considered to due to "body force" effect, inertia effect, changes in strain rate sensitivity, or a combination of them. At high velocity forming, the formability is higher than that in traditional stamping. Regazzoni et al. (1987) reported that the glide kinetics should be entirely controlled by drag under the applied stress at very high strain rates. Han and Tvergaard (1995) reported that inertia and finite strain effects are accounted for the dynamic necking of plane strain specimens under rapid deformation. Hu and Daehn (1996) showed that inertial effects are likely to be a first-order factor responsible for enhanced ductility observed in their sheet tensile tests and expanding ring tests. Seth and Daehn (2005) showed that the fragments increase with the increased strain rate in their electromagnetic expanding ring tests. However, which factor is dominant during EMF? From an overview of the-state-of-art of EMF (Psyk et al., 2011), it reveals the necessity for further consideration of these factors. One possible way is the proper decoupling of these influences. Therefore, there is a need of a forming device capable of testing standardized sheet metal specimens at speed precisely within the range of electromagnetic forming and, most importantly, their deformation can be standardized or directly compared to quasi-static and electromagnetic forming results. In this study, an impulse tension loading technique is presented. "Body force" effect and strain rate can now be separated freely by our designed device. The relation between the discharge voltage and strain rate was obtained with the help of finite element model and high-speed camera measurement results. Exploratory experiments of AA5052 Al sheet uniaxial tensile were performed at various strain rates to test the potential application of the designed instrument.

2 Experimental Design

2.1 Experimental Setup

The schematic diagram of pulsed-magnetic-driven uniaxial tension of AA5052 sheet is shown in Fig. 1. It consists of specimen, flat spiral coil, driver sheet and puller. The specimen is fixed on its one end, while the other one is attached to the puller. Fig. 1(c) shows a photograph of the experimental setup.

The driver sheet was put between coil and puller in order to accelerate the workpiece. The area of coil was covered by the driver sheet. The circle flat spiral coil is made of copper wire, with the rectangular section's dimension at 2.5×16 mm.

The specimens used in the present work were commercially available AA5052 sheets with a thickness of 1 mm. The geometry of the specimen is shown in Fig. 2. The sheet samples were prepared according to an ISO 6892: 1998. The gauged width and length of the tensile specimens were 6 and 25 mm, respectively. In order to determine the strain

distribution after testing, the surface of each sheet sample was firstly printed with 2.5 mm×2.5 mm grids. The experiments were performed using 30 kJ EMF at Harbin Institute of Technology. This system consists of a total of 14 capacitors of 192μF, which can be charged up to 5.0 kV.

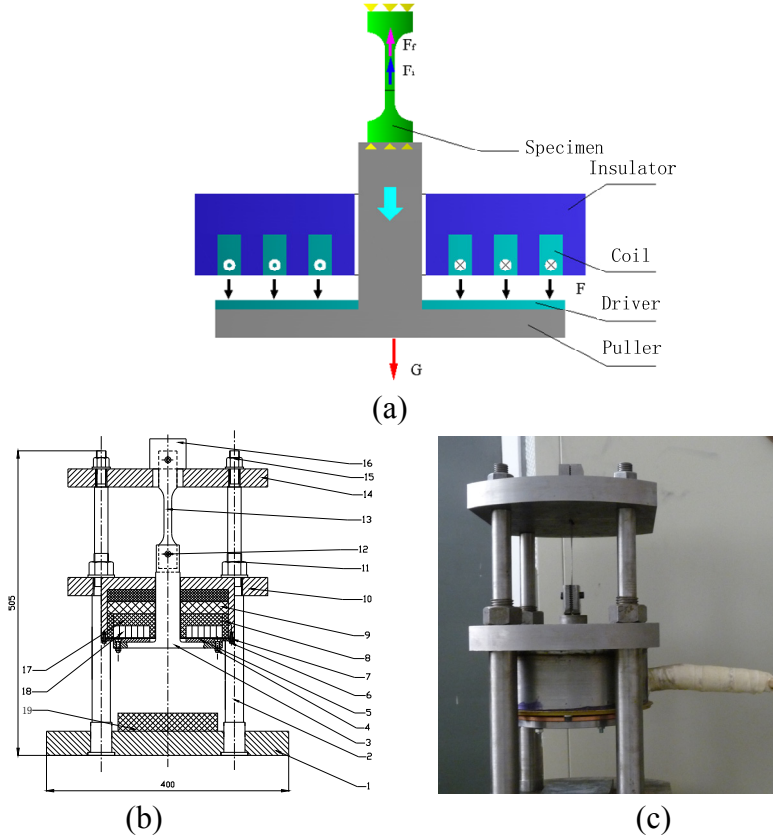

***Figure 1**: (a) Schematic of the pulsed-magnetic-driven uniaxial tension process, (b) configuration of the setup and (c) a photograph of the experimental setup.*

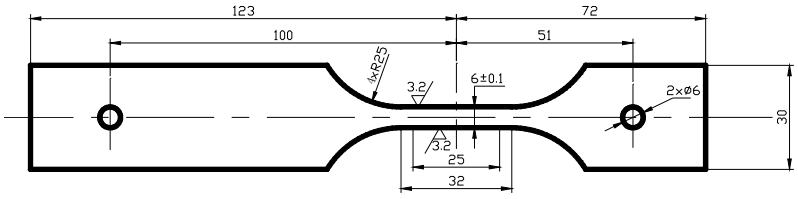

***Figure 2**: Geometry of the specimens (unit, in millimeters)*

2.2 Measurement Technique

High-speed camera (Type: FASTCAM SA5 1000K-M2) was used to obtain simultaneous high speed images of the samples during the pulsed-magnetic-driven uniaxial tension process. The images were recorded using 20 μs exposure duration. Tests were performed using the setup sketched in Fig. 3.

***Figure 3**: Pictures of high-speed camera recording the deformation of AA5052 sheet during the pulsed-magnetic-driven uniaxial tension process*

2.3 Numerical Simulation

The ANSYS FEA software was used to analyze the deformation law in pulsed-magnetic-driven uniaxial tension. ANSYS/Multiphysics was chosen to simulate the transient electromagnetic phenomena involved in the magnetic pulse forming. The mechanical behavior of the system was modeled using ANSYS/ LSDYNA, an explicit dynamic finite element program. In the simulation process, the electromagnetic field was first computed by solving theMaxwell equations, and then the Lorentz force produced by the electromagnetic model was set as the input data to calculate the deformation of the workpiece in the mechanical model. In the mechanical model, for simplicity, the coil and puller were treated as rigid bodies. In order to model the constitutive response of the material in high-strain rate, the flow stress is determined as a function of the plastic strain, the strain rate, and the temperature using the constitutive equation given by Johnson and Cook (1983):

$$\sigma = [A + B\varepsilon^n][1 + C\ln\left(\frac{\dot{\varepsilon}}{\dot{\varepsilon}_0}\right)][1 - \left(\frac{T - T_{room}}{T_{melt} - T_{room}}\right)^m] \quad (1)$$

where ε is the effective plastic strain; $\dot{\varepsilon}$ is the strain rate; $\dot{\varepsilon}_0$ is the reference strain rate; and T, Troom, and Tmelt are the absolute testing, room, and melting temperature, respectively. In this paper, A=92.4 MPa, B=132 MPa, C=0.025 and n=0.25 are the four material constants which are determined from the experimental data of AA5052 aluminum alloy. The final term on **Eq. 1**, which gives the stress an exponential decay as temperature increases, will be ignored.

3 Results and Discussion

3.1 High Speed Imaging

A sequence of high speed images showing the dynamic deformation of the AA5052 Al sheet is shown in Fig. 4. As can be seen, uniform deformation stage is about 1.3 ms at discharging voltage of 3kV and capacitor of 768μF. A necking is seen to form on the gauged length of the tensile specimen prior to fracture, as displayed in the image in Fig. 4.

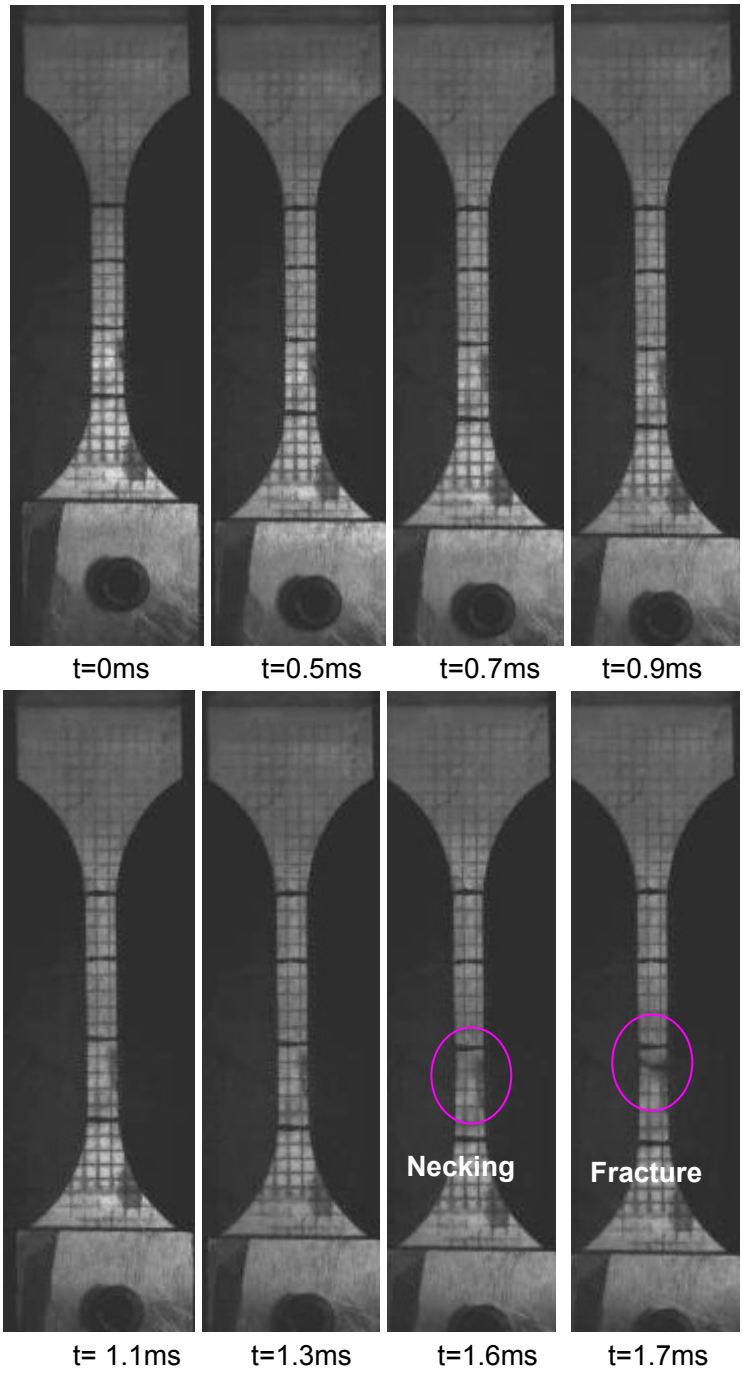

***Figure 4**: High speed image sequences showing the deformation of the AA5052 sheet sample (768uF，3kV)*

The length l of two typical points a and b on the sample was measured at different time, as shown in Fig. 5(a). The measured values of length l_i as a function of time t are plotted in Fig. 5(b). The velocity of the sample can be obtained via differential calculation. The velocity varies with the length l under the slope observation in Fig. 5(b). Here, the peak value of velocity was used in this work. The engineering strain rate can be estimated by the following equation:

$$\dot{\varepsilon}=\frac{d\varepsilon}{dt}=\frac{d(\frac{l-l_0}{l_0})}{dt}=\frac{1}{l_0}\cdot\frac{dl}{dt}=\frac{v}{l_0} \tag{2}$$

where l_0 is the original length, v is the peak value of velocity. Table 1 shows the resultant data for the velocity of puller and the strain rate, while discharge voltage is varied from 1.85kV to 3.0 kV. As can be seen, the strain rate increases with the discharge voltage at a constant capacitor of 768μF.

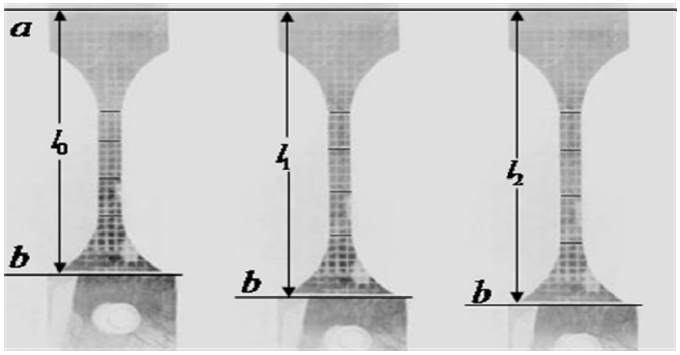

(a)

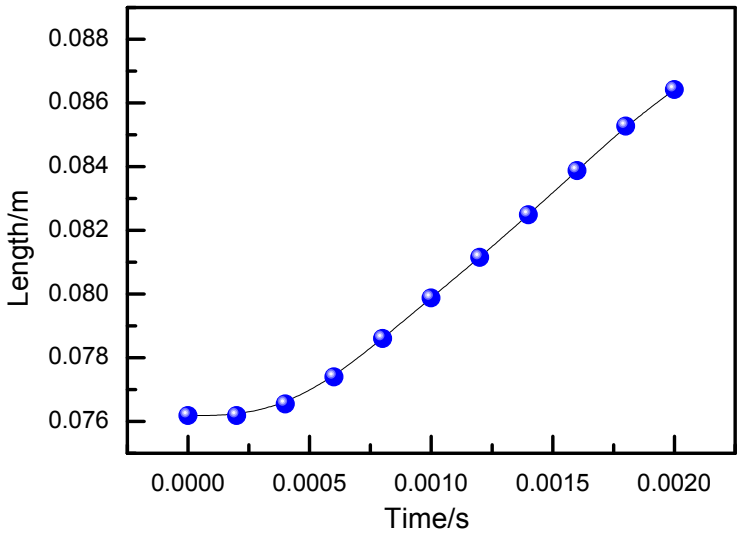

(b)

***Figure 5**: (a) The measured length l of two typical points a and b on the sample, and (b) length li as function of time t (the orginal length l0=76.18mm, 768uF, 3kV)*

***Table 1**: Velocity and strain rate for different discharge voltages*

Capacitor(μF)	Discharge voltage(kV)	Velocity(m/s)	Strain rate(s^{-1})
768	1.85	2.75	86.15
	2.00	3.05	95.41
	2.50	4.48	139.92
	2.75	5.72	178.81
	3.00	7.00	218.75

3.2 Simulation Results

Fig. 6 shows a sequence of the plastic deformation of the AA5052 Al sheet. As can be seen, deformation process predicted by simulation is similar to that observed through high-speed camera. A necking is also predicted to form in the gauged length of the tensile specimen. Figure 7 shows the velocity variation of typical elements attached to the puller at different discharge voltage and capacitor. As can be seen, the velocity increases rapidly at early stage, reaches to a maximum value and then drops gradually. The maximum value of velocity is selected to evaluate the strain rate. It should be noted that no fracture criterion was used in our current work; therefore, the velocity evolution cannot be used to predict the deform behaviour when necking occurs.

For the purpose of practical application, attempt was made to establish the relationship between the discharge voltage and strain rate. Figure 8 shows strain rate as a function of the square of discharge voltage with respect to different capacitor. For each capacitor, the point distribution shows a linear relationship between strain rate and the square of discharge voltage. As expected from the fitting formulas shown in the inset of Fig. 8, it is estimated that strain rate can range from $130s^{-1}$ to $3267s^{-1}$ by our developed setup, as discharge voltage varies from 1kV to 5kV at a constant capacitor of 1920μF.

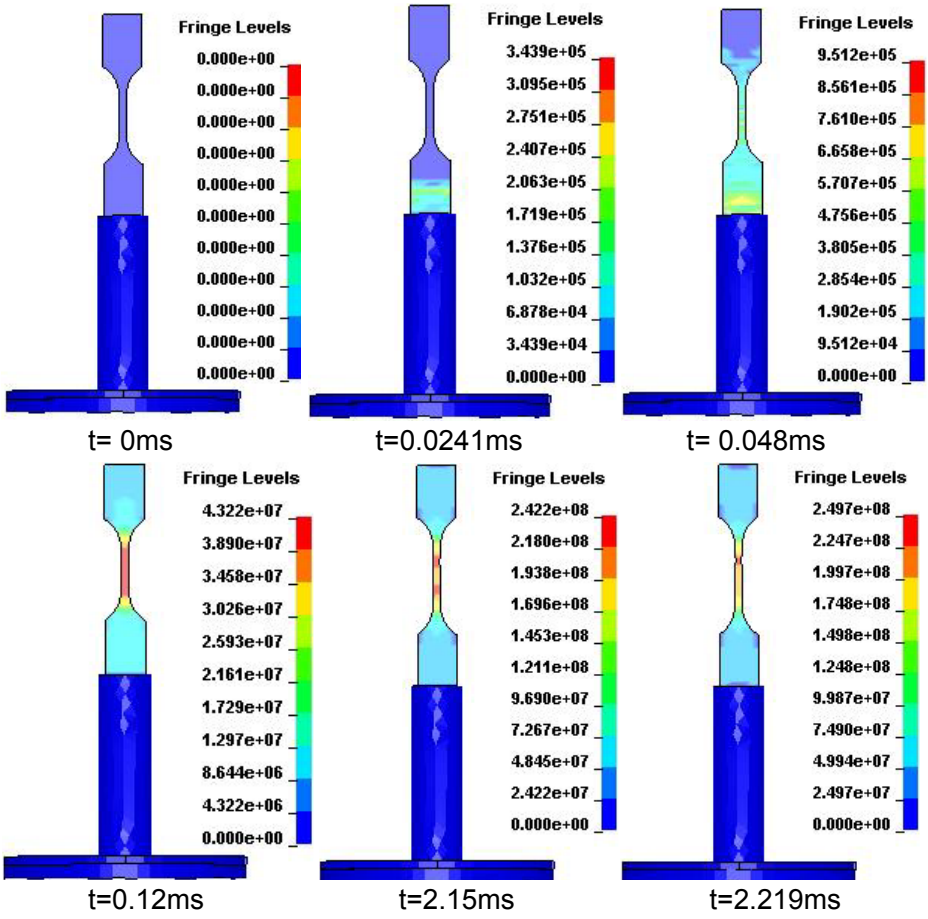

***Figure 6**: Von Mises stress evolution pridicted by numerical simulation (768uF，3kV)*

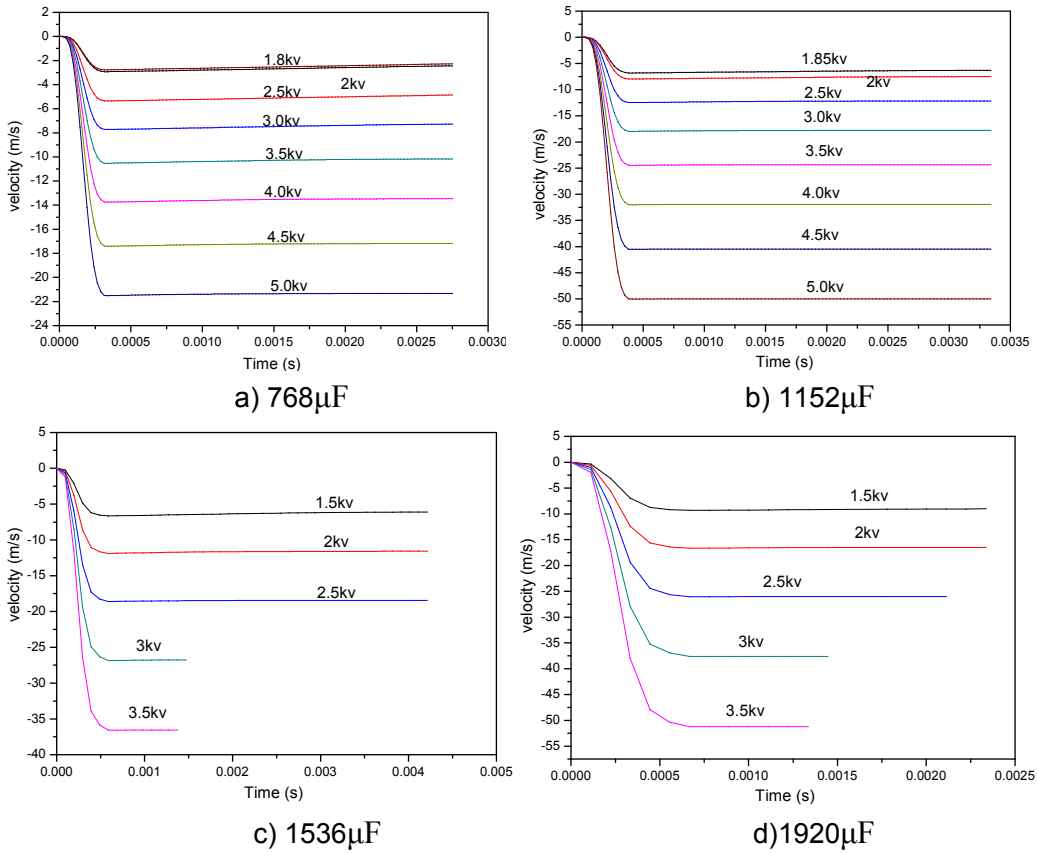

***Figure 7**: Velocity as a function of discharge voltage for four select values of the capacitor: (a) 768μF; (b) 1152μF; (c) 1536μF and (d) 1920μF*

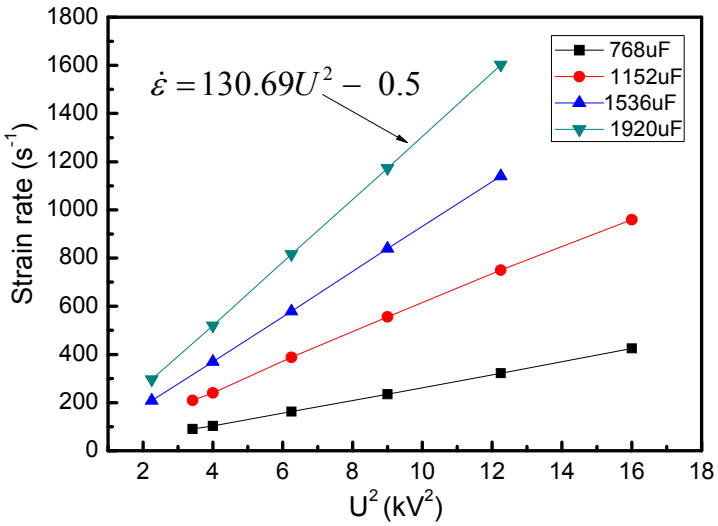

***Figure 8**: Strain rate as a function of the square of discharge voltage with respect to different capacitor*

3.3 Experimental Results

For verification purposes, strain rate predicted by simulation was compared to experimental one. Fig.9 displays the comparison results for four selected value of discharge voltage at a constant capacitor of 768μF. It is observed that the errors between the measured and calculated results are less than 10%. The little deviation may be due to the loosely couple method used in this work. The experimental and simulation results have a good agreement. Therefore, one can safely use the relationship between the strain rate and discharge voltage established by simulation.

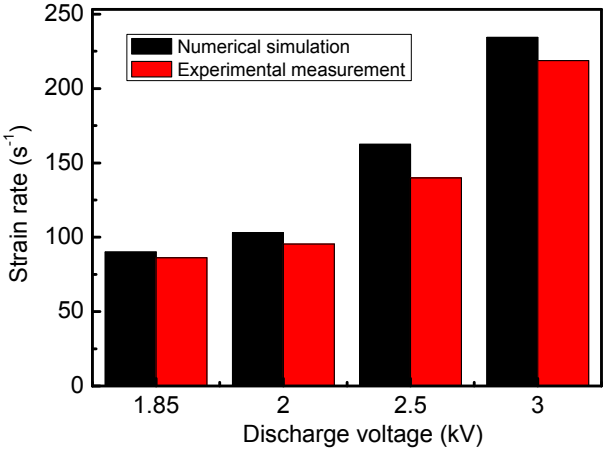

***Figure 9**: Comparison of analytically predicted and experimentally determined strain rate (768μF)*

Experiments of uniaxial tensile were then performed on the designed instrument at various strain rates to investigate the deformation behaviour of AA5052 Al sheet. Fig. 10 shows the deformed samples at different discharge voltage for two selected values of capacitor. It was found that ductility of tensile specimen increases, as the test velocity increases. The results show that the developed instrument is capable of testing standardized sheet metal specimens at speed precisely within the range of electromagnetic forming. What's more, their deformation can be directly compared to quasi-static results.

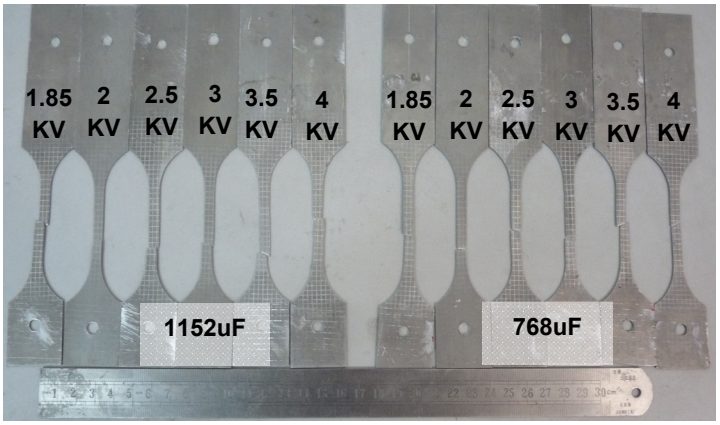

***Figure 10**: Deformed samples of 5052 Al after EMF with different discharge voltage for two selected value of capacitor*

Conclusion

An impulse tension loading technique is presented, which is based on the use of pulsed-magnetic-driven tension loading. The developed setup can provide reproducible and adjustable loading rate ($80s^{-1}$~$3267s^{-1}$) via the discharge voltage and capacitance. The relation between discharge voltage and strain rate obtained from finite element calculations can be used for the process design. It could be a valuable technique for an investigation of material dynamic response. Also, it is worth to note that more technical details still need to be solved, such as how to measure the force accurately in the designed device.

Acknowledges

This work was supported by the National Basic Research Program of China (2011CB012805), which is gratefully acknowledged here.

References

Han, J. B., & Tvergaard, V., 1995. Effect of inertia on the necking behaviour of ring specimens under rapid radial expansion. European journal of mechanics. A. Solids, 14(2), 287-307.

Hu, X., & Daehn, G. S., 1996. Effect of velocity on flow localization in tension. Acta Materialia, 44(3), 1021-1033.

Johnson G., Cook W., 1983. A constitutive model and data for metals subjected to large strains, high strain rates and high temperatures, In: Proceedings of 7th International Conference on Ballistics, pp 541–547.

Psyk, V., Risch, D., Kinsey, B.L., Tekkaya, A.E., Kleiner, M., 2011. Electromagnetic forming – A review. Journal of Materials Processing Technology 211 (5), pp. 787-829.

Regazzoni, G., Kocks, U. F., & Follansbee, P., 1987. Dislocation kinetics at high strain rates. Acta metallurgica, 35(12), 2865-2875.

Seth, M., & Daehn, G. S., 2005. Effect of aspect ratio on high velocity formability of aluminum alloy. Trends in Materials and Manufacturing Technologies for Transportation Industries.